



Partial Duality of Hypermaps

S. Chmutov¹ · F. Vignes-Tourneret²

Received: 9 February 2021 / Revised: 6 October 2021 / Accepted: 9 November 2021 /
Published online: 3 January 2022
© Institute for Mathematical Sciences (IMS), Stony Brook University, NY 2021

Abstract

We introduce partial duality of hypermaps, which include the classical Euler–Poincaré duality as a particular case. Combinatorially, hypermaps may be described in one of three ways: as three involutions on the set of flags (bi-rotation system or τ -model), or as three permutations on the set of half-edges (rotation system or σ -model in orientable case), or as edge 3-coloured graphs. We express partial duality in each of these models. We give a formula for the genus change under partial duality.

Keywords Maps · Hypermaps · Partial duality · Permutational models · Rotation system · Bi-rotation system · Edge-coloured graphs

Mathematics Subject Classification 05C10 · 05C65 · 57M15 · 57Q15

Contents

Introduction	446
1 Hypermaps	447
2 Partial Duality	455
3 Genus Change	464
4 Directions of Future Research	466
References	467

✉ F. Vignes-Tourneret
vignes@math.univ-lyon1.fr

S. Chmutov
chmutov@math.ohio-state.edu

¹ The Ohio State University, Mansfield Campus, 1760 University Drive, Mansfield, OH 44906, USA

² Univ Lyon, CNRS, Université Claude Bernard Lyon 1, UMR 5208, Institut Camille Jordan, 69622 Villeurbanne, France

Introduction

Maps can be thought of as graphs embedded into surfaces. *Hypermaps* are hypergraphs embedded into surfaces. In other words, in hypermaps, a (hyper) edge is allowed to connect more than two vertices, so having more than two *half-edges*, or just a single half-edge (see Fig. 1).

One combinatorial description of hypermaps, called the *bi-rotation system* or the τ -model, goes through three involutions acting on the set of *local flags*, also known as *blades*, represented by triples (vertex, edge, face). The motivation for this model was the study of symmetry of regular polyhedra which is a group generated by reflections (involutions). As such, it may be traced back to Ancient Greeks. It was used systematically by Klein [23] and later by Coxeter and Moser [5]. More recently, this model was used in the context of maps and hypermaps in [20–22,39]. We review the τ -model in Sect. 1.2.

Another way to combinatorially study oriented hypermaps, called the *rotation system* or the σ -model, is to consider permutations of its half-edges, also known as *darts*, around each vertex, around each hyperedge, and around each face according to the orientation. This model has been carefully worked out by Cori [6]; however, it can be traced back to Heffter [18]. It became popular after the work of Edmonds [8]. It is very important for the Grothendieck *dessins d’Enfants* theory, see [27], where the σ -model is called *3-constellation*. We review the σ -model in Sect. 1.3.

In 1975, Walsh noted [38] that, if we consider a small regular neighbourhood of vertices and hyperedges, then we can regard hypermaps as cell decomposition of a compact closed surface into disks of three types, vertices, hyperedges, and faces, such that the disks of the same type do not intersect and the disks of different types may intersect only on arcs of their boundaries. These arcs form a 3-regular graph whose edges are coloured in 3 colours depending on the types of cells they are adjacent to. The arcs of intersection of hyperedge-disks with face-disks bear the colour 0. The colour 1 stands for the arcs of intersection of vertex-disks with face-disks. And the arcs of intersection of vertex-disks with hyperedge-disks are coloured by 2. Thus, we come to the concept of [2]-coloured graphs, where [2] stands for the set of three colours $[2] := \{0, 1, 2\}$. It turns out that such a [2]-coloured graph carries all the information about the original hypermap. This gives another combinatorial model for description of hypermaps. We review this model in Sect. 1.4.

About the same time, this concept was generalized to higher dimensions. Namely, in the 1970s, Pezzana [31,32] discovered a way of coding a piecewise-linear (PL) manifold by a properly edge-coloured graph. The idea goes as follows: choose a triangulation K of this given manifold M . Consider then its first barycentric subdivision K_1 . The 1-skeleton of K_1^* is a properly edge-colourable graph. It turns out that the colouring of the graph is sufficient to reconstruct M completely. The discovery of Pezzana allows to bring combinatorial and graph theoretical methods into PL topology. This correspondence between PL manifolds and coloured graphs has been further developed by Ferri, Gagliardi, and their group [12]. It has also been independently rediscovered by Vince [35], Lins and Mandel [26], and, to a certain extent, Gurau [16].

Originally, partial duality relative to a subset of edges was defined for ribbon graphs in [3] under the name of generalized duality. The motivation came from an idea to

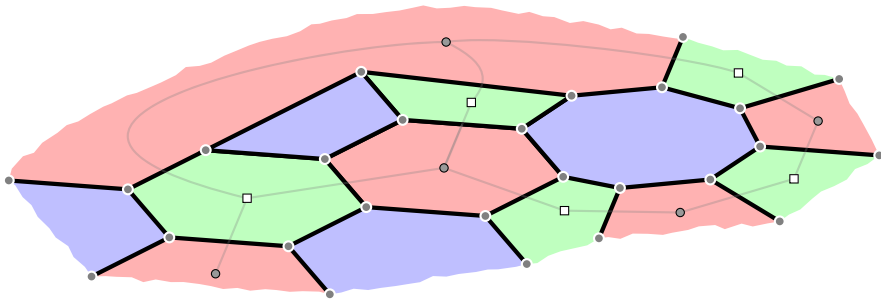


Fig. 1 Local view of a hypermap with its Walsh map superimposed (vertices are red, hyperedges are green, and faces are blue)

unify various versions of the Thistlethwaite theorems in knot theory relating the Jones polynomial of knots with the Tutte-like polynomial of (ribbon) graphs. Then, it was thoughtfully studied and developed in papers [1,9,13,19,28–30,37]. We refer to [10] for an excellent account on this development.

The main result of this paper is a generalization of partial duality to hypermaps in Sect. 2. There, we define the partial duality in Sect. 2.1 and then describe it in each of the three combinatorial models in subsequent subsections. Independently, this generalization was found by Benjamin Smith [33], but it does not contain the expression of partial duality in terms of permutational models and does not have any formula for the genus change. The operation of partial duality usually is different from the operations of [21,22] and from the operation of [36]. Typically, it changes the genus of a hypermap. We give a formula for the genus change in Sect. 3. We finish the paper with general remarks about future directions of research on partial duality in higher dimensions.

1 Hypermaps

1.1 Geometrical Model

A *map* is a cellularly embedded graph in a (not necessarily orientable) compact closed surface. The edges of a graph are represented by smooth arcs on the surface connecting two (not necessarily distinct) vertices. A small regular neighbourhood of such a graph on the surface is a surface with boundary, called *ribbon graph*, equipped with a decomposition into a union of topological disks of two types, the neighbourhoods of vertices and the neighbourhoods of edges. The last one can be regarded as a narrow quadrilateral along the edges attached to the corresponding vertex-disks at the two opposite sides. Attaching disks called *faces* to the boundary components of a ribbon graph restores the original closed surface. Thus, a map may be regarded as a cell decomposition of a compact closed surface into disks of three types, vertices, edges, and faces, such that the disks of the same type do not intersect and the disks of different types may intersect only on arcs of their boundaries and the edge-disks intersect with at most two vertex-disks and at most two face-disks (see [10] for example).

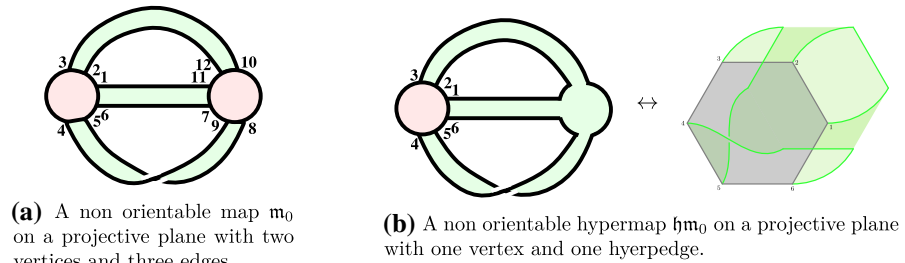


Fig. 2 Map and hypermap

Hypermaps differ from maps in that the edges are allowed to be *hyperedges* and may connect several vertices. Let us consider a graph, the vertices of which are coloured black say. Subdivide each of its edges by adding a white vertex at its center. A graph is thus equivalent to a bipartite graph; all the vertices of one class of its bipartition are of degree 2. A hypergraph is then equivalent to a (general) bipartite graph. Hypermaps may be considered as cellularly embedded hypergraphs. Moreover, hypermaps can also be defined as cell decomposition of a compact closed surface into disks of three types, vertices, hyperedges, and faces, such that the disks of the same type do not intersect and the disks of different types may intersect only on arcs of their boundaries. In contrast with maps, edge-disks of hypermaps need not be quadrilaterals. Therefore, the definition of a hypermap is completely symmetrical with respect to the types of the cells. Figure 2 shows a non orientable map m_0 and a hypermap hm_0 obtained from m_0 by uniting the right vertex with the three edges into a single hyperedge.

As abstract surfaces, both m_0 and hm_0 are homeomorphic to a Möbius band with a hole in it (a cycle labeled by $1 - 2 - 1_2 - 1_1$ on m_0). Therefore, gluing two disks (faces) to its boundary components, we will get a projective plane.

1.2 Permutational τ -Model

In this model, also called *bi-rotation system*, a hypermap hm is described in a pure combinatorial way as three fixed point-free involutions, $\tau_0, \tau_1,$ and $\tau_2,$ acting on a set X of *local flags* of hm . A (local) flag is a triple (v, e, f) consisting of a vertex v , the intersection e of a hyperedge incident to v with a small neighbourhood of v , and the intersection f of a face adjacent to v and e with the same neighbourhood of v . Another way of defining a local flag is to consider a triangle in the barycentric subdivision of faces of hm considered as an embedded hypergraph. We will depict a flag as a small

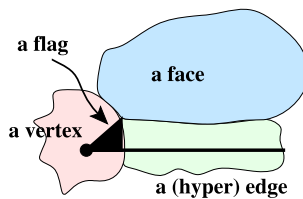


Fig. 3 A local flag

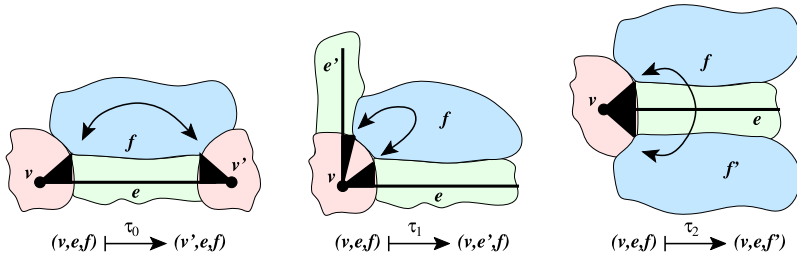


Fig. 4 Involutions τ_0, τ_1, τ_2

black right triangle with one acute angle at v , another one at a point where all three disks v, e , and f meet and a right angle at an arc of intersection of disks v and e (Figs. 3, 4).

When a hypermap is understood as a [2]-coloured cell decomposition of a surface, the local flags correspond to the points where all three types of cells meet together. Three lines of cell intersections emanate from each such point, the 2-line of intersection of the vertex-disk with the (hyper) edge-disk, the 1-line of intersection of the vertex-disk with the face-disk, and the 0-line of intersection of the edge-disk with the face-disk. These lines yield three partitions of the set X of local flags into pairs of flags whose corresponding points are connected by 0-, 1-, or 2-lines. The permutation τ_i swaps the flags in the pairs connected by the i -lines.

In Fig. 2, the local flags are labeled by numbers. For these hypermaps, the permutations τ_i are the following. For the map m_0

$$\begin{aligned} \tau_0 &= (1, 11)(2, 12)(3, 10)(4, 9)(5, 8)(6, 7), \\ \tau_1 &= (1, 2)(3, 4)(5, 6)(7, 9)(8, 10)(11, 12), \\ \tau_2 &= (1, 6)(2, 3)(4, 5)(7, 11)(8, 9)(10, 12). \end{aligned}$$

For hm_0

$$\tau_0 = (1, 2)(3, 5)(4, 6), \quad \tau_1 = (1, 2)(3, 4)(5, 6), \quad \tau_2 = (1, 6)(2, 3)(4, 5).$$

Any three fixed point-free involutions on a set X yield a hypermap. Its vertices correspond to orbits of the subgroup $\langle \tau_1, \tau_2 \rangle$ generated by τ_1 and τ_2 , edges to the orbits of $\langle \tau_0, \tau_2 \rangle$, and faces to the orbits of $\langle \tau_0, \tau_1 \rangle$. A hyperedge is a genuine edge if the corresponding orbit consists of four elements. Thus, a hypermap is a map if and only if $\tau_0\tau_2$ is also an involution.

Remark Tutte [34] introduced a less symmetrical description of combinatorial maps in terms of three permutations θ, ϕ , and P . They can be expressed in terms of τ_0, τ_1 , and τ_2 as follows:

$$\theta = \tau_2, \quad \phi = \tau_0, \quad P = \tau_1\tau_2.$$

1.3 Permutational σ -Model

This model, also known as *rotation system*, gives a presentation of an oriented hypermap in terms of three permutations σ_V, σ_E , and σ_F of its *half-edges* H satisfying the

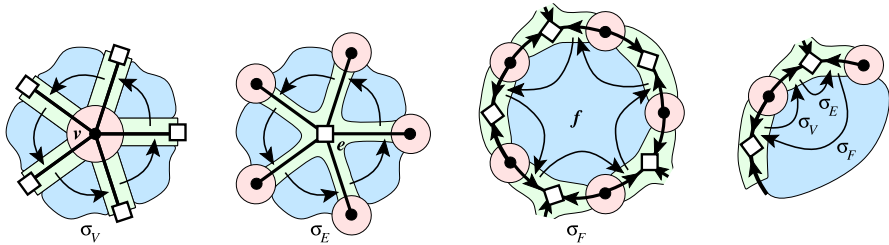


Fig. 5 Permutations $\sigma_V, \sigma_E, \sigma_F$, and the identity $\sigma_F\sigma_E\sigma_V = 1$

relation $\sigma_F\sigma_E\sigma_V = 1$. We may think of half-edges as non complete local flags (v, e) consisting of a vertex v and the intersection e of a hyperedge incident to v with a small neighbourhood of v . Therefore, a genuine edge has two half-edges, but a hyperedge may have more than two half-edges or even a single half-edge. If we think of a hypermap as an embedded bipartite graph, then the hyperedges of the hypermap precisely correspond to the edges of the bipartite graph. In the following, we place an empty square at the center of the hyperedge to distinguish it from a vertex.

The permutation σ_V is a cyclic permutation of half-edges incident to a vertex according to the orientation of the hypermap. The permutation σ_E acts as the cyclic permutation of rays in each star according to the orientation. For the permutation σ_F , we need to direct the half-edges with arrows pointing away from the vertices to which they are attached. These arrows point toward the centers of the stars of the hyperedges. The permutation σ_F cyclically permutes those half-edges in each face which are directed along the orientation of the face.

One can easily check that $\sigma_F\sigma_E\sigma_V = 1$, see Fig. 5. The cycles of σ_V correspond to the vertices of the hypermap, the cycles of σ_E correspond to the hyperedges, and the cycles of σ_F correspond to the faces of the hypermap. Consequently any three permutations σ_V, σ_E , and σ_F of a set H satisfying the relation $\sigma_F\sigma_E\sigma_V = 1$ uniquely determine an oriented hypermap.

Now, let us describe the relation with the τ -model of Sect. 1.2. Each half-edge has two local flags in which it participates. If $x \in X$ is one of them, then $\tau_2(x)$ is the other one. Therefore, the cardinality of H is twice smaller that the cardinality of X .

Suppose an oriented hypermap $\mathfrak{h}m$ is given by its σ -model on the set of half-edges $H = \{1, \dots, m\}$. We set X to be a double of H , $X := \{1_-, 1_+, 2_-, 2_+, \dots, m_-, m_+\}$, and the involution τ_2 to swap i_- and i_+ . Define the permutation τ_0 to be $\tau_0(i_-) := (\sigma_E(i))_+$ and $\tau_0(i_+) := (\sigma_E^{-1}(i))_-$. Finally, define τ_1 as $\tau_1(i_-) := (\sigma_V^{-1}(i))_+$ and $\tau_1(i_+) := (\sigma_V(i))_-$. Obviously, they are involutions and the hypermap they define is $\mathfrak{h}m$.

In the opposite way, suppose a hypermap $\mathfrak{h}m$ is given by its τ -model on the set of local flags $X = \{1, \dots, n\}$. Also, suppose that $\mathfrak{h}m$ is *connected*. That means the group generated by τ_0, τ_1 , and τ_2 acts transitively on X .

For an orientable hypermap, we can consistently arrange X in pairs with subscripts $+$ and $-$ as in Fig. 6. For a nonorientable hypermap, such an arrangement is impossible. One may observe that τ s always change the subscript to the opposite one. This means that the subgroup G of words of even length in τ 's preserve the subscript. The group

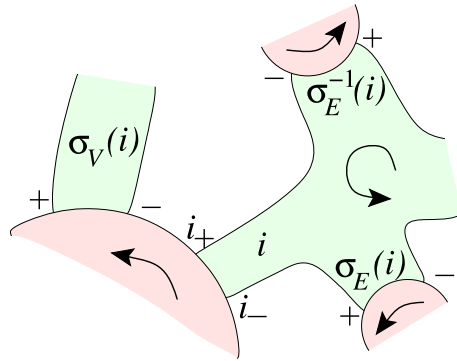


Fig. 6 σ and τ permutations

G is generated by $\tau_2\tau_1$, $\tau_0\tau_2$, and $\tau_1\tau_0$. For a nonorientable hypermap, the subgroup G also acts transitively on X . In the orientable case, X splits into two orbits of G , one with the subscript $+$ and another one with the subscript $-$. Let H be the one with subscript $+$. Then, we set σ_V (resp. σ_E and σ_F) to be the restriction of $\tau_2\tau_1$ (resp. $\tau_0\tau_2$, and $\tau_1\tau_0$) on the orbit H . Obviously, these restrictions satisfy the relation $\sigma_F\sigma_E\sigma_V = (\tau_1\tau_0)(\tau_0\tau_2)(\tau_2\tau_1) = 1$. It is clear from Fig. 6 that the σ -model constructed in this way gives the original orientable hypermap $\mathfrak{h}m$. The restriction to the “ $-$ ”-orbit gives the same hypermap with the opposite orientation.

Example 1 For hypermaps on Fig. 2, the subgroup G is generated by the following permutations. For m_0

$$\begin{aligned} \tau_2\tau_1 &= (1, 3, 5)(2, 6, 4)(7, 8, 12)(9, 11, 10), \\ \tau_0\tau_2 &= (1, 7)(2, 10)(3, 12)(4, 8)(5, 9)(6, 11), \\ \tau_1\tau_0 &= (1, 12)(2, 11)(3, 8, 6, 9)(4, 7, 5, 10). \end{aligned}$$

For $\mathfrak{h}m_0$, $\tau_2\tau_1 = (1, 3, 5)(2, 6, 4)$, $\tau_0\tau_2 = (1, 4, 3)(2, 5, 6)$, $\tau_1\tau_0 = (1, 2)(3, 6)(4, 5)$. In both cases, the group G acts transitively on flags. This is a combinatorial expression of the fact that these two hypermaps are non orientable.

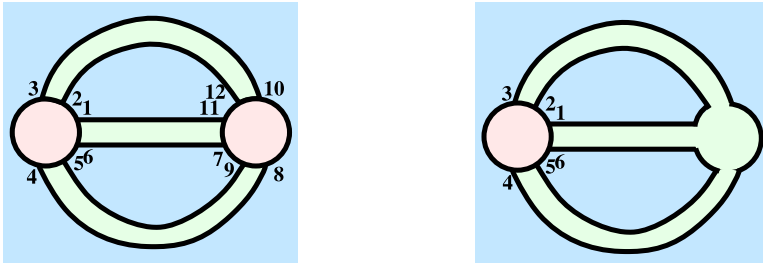
On the contrary, consider the two oriented hypermaps of Fig. 7.

The permutations τ_i are the following. For the map m_1

$$\begin{aligned} \tau_0 &= (1, 11)(2, 12)(3, 10)(4, 8)(5, 9)(6, 7), \\ \tau_1 &= (1, 2)(3, 4)(5, 6)(7, 9)(8, 10)(11, 12), \\ \tau_2 &= (1, 6)(2, 3)(4, 5)(7, 11)(8, 9)(10, 12). \end{aligned}$$

For $\mathfrak{h}m_1$, $\tau_0 = (1, 2)(3, 4)(5, 6)$, $\tau_1 = (1, 2)(3, 4)(5, 6)$, $\tau_2 = (1, 6)(2, 3)(4, 5)$. The generators of the subgroup G for m_1 are

$$\tau_2\tau_1 = (1, 3, 5)(2, 6, 4)(7, 8, 12)(9, 11, 10),$$



(a) An orientable map m_1 on a sphere with two vertices and three edges

(b) An orientable hypermap hm_1 on a sphere with one vertex and one hyperedge

Fig. 7 Map and hypermap. Second example

$$\begin{aligned} \tau_0\tau_2 &= (1, 7)(2, 10)(3, 12)(4, 9)(5, 8)(6, 11), \\ \tau_1\tau_0 &= (1, 12)(2, 11)(3, 8)(4, 10)(5, 7)(6, 9). \end{aligned}$$

For hm_1 : $\tau_2\tau_1 = (1, 3, 5)(2, 6, 4)$, $\tau_0\tau_2 = (1, 5, 3)(2, 4, 6)$, $\tau_1\tau_0 = 1$. One can see that the group G has two orbits on the set of flags. The “+”-orbits are: for m_1 , $H = \{1, 3, 5, 7, 8, 12\}$; for hm_1 , $H = \{1, 3, 5\}$. The restriction of the generators on this orbit gives the σ -models.

For m_1 : $\sigma_V = (1, 3, 5)(7, 8, 12)$, $\sigma_E = (1, 7)(3, 12)(5, 8)$, $\sigma_F = (1, 12)(3, 8)(5, 7)$.
 For hm_1 : $\sigma_V = (1, 3, 5)$, $\sigma_E = (1, 5, 3)$, $\sigma_F = 1$.

There is an elegant formula for the Euler characteristic of a hypermap in terms of its σ -model.

Lemma 1.1 [27, Proposition 1.5.3] *Let $hm = (\sigma_V, \sigma_E, \sigma_F)$ be an oriented hypermap given by its σ model on the set H of n half-edges, $n := \#H$. Let c_V (resp. c_E and c_F) denote the number of cycles of σ_V (resp. σ_E and σ_F). Then, the Euler characteristic $\chi(hm)$ of the surface of hm is equal to*

$$\chi(hm) = c_V + c_E + c_F - n.$$

Proof Let \mathcal{T} be the cell decomposition (tessellation) given by the hypermap hm .

Note that

- $2n$ is the number of vertices of \mathcal{T} ;
- the number of polygons in \mathcal{T} is $c_V + c_E + c_F$;
- the number of edges of \mathcal{T} is $3n$.

Then, the formula follows. □

1.4 Edge-Coloured Graphs

As indicated in Sect. 1.2, the boundaries of cells of a hypermap form a 3-regular graph embedded into the surface of the hypermap. It carries a natural edge colouring: the arcs of intersection of hyperedges and faces are coloured by 0, the arcs of intersection

of vertices and faces are coloured by 1, and the arcs of intersection of vertices and hyperedges are coloured by 2. In this subsection, we show that the entire hypermap can be reconstructed from this information.

Definition 1.2 Let κ be a finite set. A κ -coloured graph is an abstract connected graph, such that each edge carries a “colour” in κ and each vertex is incident to exactly one edge of each colour.

Note that a κ -coloured graph is necessarily $\#\kappa$ -regular and has no loops (but may contain multiple edges). In the following, for all $I \subset \kappa$, we will denote $\kappa \setminus I$ by \bar{I} .

Let $\kappa = \{1, 2, \dots, \#\kappa\}$. For a κ -coloured graph Γ , we can define a permutational τ -model as a set of involutions $\tau_1, \tau_2, \dots, \tau_{\#\kappa}$ acting on the set X of vertices of Γ as follows. τ_i interchange the vertices connected by an edge of colour i . For the coloured graphs coming from hypermaps, these permutations coincide with the τ -model from Sect. 1.2.

Each coloured graph Γ contains some special coloured subgraphs called *bubbles* in [16] and *residues* in [35].

Definition 1.3 Let Γ be a κ -coloured graph and $I \subset \kappa$. An *#I-bubble* of colours I in Γ is a connected component of the I -coloured subgraph of Γ induced by the edges of Γ with colours in I .

In particular, 0-bubbles, corresponding to $I = \emptyset$, are the vertices of Γ . The set of bubbles in Γ of colours $I \subset \kappa$ is denoted by $\mathcal{B}^I(\Gamma)$ or \mathcal{B}^I if there is no ambiguity. B^I is its cardinality $\#\mathcal{B}^I$. We also define $\mathcal{B}_n(\Gamma)$, $0 \leq n \leq \#\kappa - 1$, to be the set of all n -bubbles in Γ : $\mathcal{B}_n := \bigcup_{I \subset \kappa, \#I=n} \mathcal{B}^I$ and $B_n := \#\mathcal{B}_n$. Finally, the whole set of bubbles of Γ , $\bigcup_{0 \leq n \leq \#\kappa - 1} \mathcal{B}_n$, is written as $\mathcal{B}(\Gamma)$. The subgraph inclusion relation provides $\mathcal{B}(\Gamma)$ with a poset structure.

1.4.1 Topology of Edge-Coloured Graphs

To each coloured graph Γ , one can associate two cell complexes, $\Delta^*(\Gamma)$ and its (“Poincaré”) dual $\Delta(\Gamma)$, as follows.

For each $D \in \mathbb{N}$, let $[D]$ be the set $\{0, 1, \dots, D\}$.

The dual complex $\Delta^*(\Gamma)$. Let Γ be a $[D]$ -coloured graph. To each D -bubble $b \in \mathcal{B}^{[\bar{D}]}$ (Γ), one associates a 0-simplex $\mathfrak{s}(b)$ coloured i . To each $(D - 1)$ -bubble $b \in \mathcal{B}^{[\bar{i}, \bar{j}]}$, one associates an edge $\mathfrak{s}(b)$, the endpoints of which are, respectively, coloured i and j . In general, to each k -bubble $b \in \mathcal{B}^{[\bar{i}_1, \dots, \bar{i}_k]}$, one associates an abstract $(D - k)$ -simplex $\mathfrak{s}(b)$ coloured $[D] \setminus \{i_1, \dots, i_k\}$. Now, the poset structure of $\mathcal{B}(\Gamma)$ provides gluing data for those simplices. Indeed, let us consider two $(D - k)$ -simplices $\mathfrak{s}(b)$ and $\mathfrak{s}(b')$. If the corresponding k -bubbles b and b' are contained in a common $(k + 1)$ -bubble b'' , identify $\mathfrak{s}(b)$ and $\mathfrak{s}(b')$ along their common facet $\mathfrak{s}(b'')$. This gluing respects the colouring structure of the simplices. It can be shown that such a complex is a trisp (for triangulated space) [24]. Vince [35, p.4] called the topological space of this simplicial complex the *underlying topological space of the combinatorial map* Γ . However, there is also another complex associated with Γ , dual to Δ^* .

The direct complex $\Delta(\Gamma)$. It is constructed inductively, like a CW complex. To each k -bubble, $0 \leq k \leq D$, one will associate a k -dimensional topological space. To

each 0-bubble b , i.e. to each vertex of Γ , corresponds a point $|b|$. Each edge e of Γ , i.e., each 1-bubble, contains two vertices u and v . Define $|e|$ as the cone over $|u| \cup |v|$. The realization $|e|$ of e is thus a segment. Now, consider a 2-bubble b . It is a bicoloured cycle in Γ . b contains a set of edges whose realization forms a circle. $|b|$ is defined as a cone over this circle hence a 2-disk. In general, let b be k -bubble. It contains a set $\mathcal{B}_{k-1}(b)$ of $(k - 1)$ -bubbles. The realization of any $b' \in \mathcal{B}_{k-1}(b)$ has been defined at the previous induction step. The realizations $|b_1|$ and $|b_2|$ for $b_1, b_2 \in \mathcal{B}_{k-1}$ are identified along $|b_1 \cap b_2|$ (which is a union of lower dimensional bubbles). Then, the whole set $\mathcal{B}_{k-1}(b)$ has a (connected) realization that we denote $\partial|b|$. Finally, $|b|$ is defined as the cone over $\partial|b|$ (hence the name).

In fact, one can prove that the union of the realizations of the $(k - 1)$ -sub-bubbles of a given k -bubble b is homeomorphic to the link of $\mathfrak{s}(b)$ in $\Delta^*(\Gamma)$. Therefore, the realization of b is homeomorphic to the dual block of $\mathfrak{s}(b)$ in the first barycentric subdivision of $\Delta^*(\Gamma)$.

The realization $|\Gamma|$ of Γ corresponds to the gluing of the D -blocks of $\Delta(\Gamma)$. $\Delta(\Gamma)$ is a complex whose blocks are topological spaces glued along their common boundaries. However, in general, its blocks are not homeomorphic to balls. And indeed, $|\Gamma|$ is generally not a manifold but a normal pseudo-manifold [17].

1.4.2 Hypermaps as Edge-Coloured Graphs

It was mentioned at the beginning of this subsection that a hypermap $\mathfrak{h}\mathfrak{m}$ determines a [2]-coloured graph $\Gamma_{\mathfrak{h}\mathfrak{m}}$. Its vertices corresponds to (local) flags of $\mathfrak{h}\mathfrak{m}$ and its edges of colour i correspond to the orbits of the involution τ_i .

Here is an inverse construction. Let us consider a [2]-coloured graph Γ . The 2-cells of its direct complex $\Delta(\Gamma)$ are polygons and $|\Gamma|$ is thus the result of the gluing of polygons along common boundaries. Randomly gluing polygons along edges does not generally produce manifolds. However, the gluing of polygons, *dictated by a coloured graph*, is always a manifold and thus a closed compact (not necessarily orientable) surface. Moreover, those polygons are of three types: they are bounded by either 01-, 02-, or 12-cycles (2-bubbles). Said differently, $\Delta(\Gamma)$ is, in dimension 2, a polygonal tessellation of a closed compact (not necessarily orientable) surface with polygons of three different types, i.e., a hypermap $\mathfrak{h}\mathfrak{m}$. Thus, [2]-coloured graphs provide another description of hypermaps (Fig. 8).

In the case of maps, namely when all 02-cycles are of length 4, the [2]-coloured graphs are also known as graph-encoded maps [25].

Example 2 Here are the examples of [2]-coloured graphs for hypermaps $\mathfrak{h}\mathfrak{m}_0$ from Fig. 2 and $\mathfrak{h}\mathfrak{m}_1$ from Fig. 7.

A reader may enjoy constructing the direct complexes $\Delta(\Gamma_{\mathfrak{h}\mathfrak{m}_0})$ and $\Delta(\Gamma_{\mathfrak{h}\mathfrak{m}_1})$, and checking that they are indeed isomorphic to the hypermaps from Figs. 2 and 7.

Lemma 1.4 *A hypermap corresponding to a [2]-coloured graph Γ is orientable if and only if Γ is bipartite.*

The proof of this goes back to [2]. The maps case can also be found in [25].

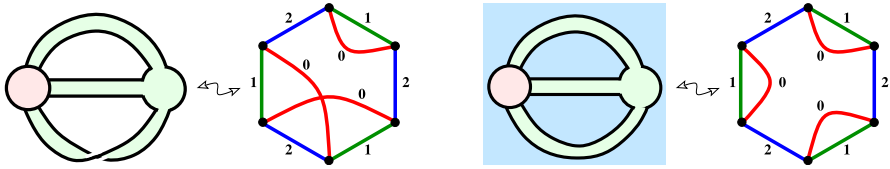


Fig. 8 [2]-coloured graphs Γ_{hm_0} and Γ_{hm_1}

Proof According to Sect. 1.3, a hypermap is orientable if and only if the vertices of Γ can be split into two parts with subscripts $+$ and $-$ as in Fig. 6. \square

Remark In [35], A. Vince proposed a way to associate a $[d]$ -coloured graph Γ to any cell decomposition K of a closed d -manifold. Γ is defined as the 1-skeleton of the complex dual to the first barycentric subdivision of K . Whereas his method works for any cell complex associated to closed manifolds, it does not define a one-to-one correspondence between hypermaps and [2]-coloured graphs (not all coloured graphs have a dual complex which is the barycentric subdivision of another cell complex). Moreover, the coloured graph thus associated with K is of higher order than ours.

2 Partial Duality

2.1 Definition

Assume that a hypermap hm is connected. Otherwise, we will need to do partial duality for each connected component separately and then take the disjoint union. Let S be a subset of cells of hm of the same type, either vertex-cells, or hyperedge-cells, or face-cells. We will define the *partial dual hypermap* hm^S relative to S . If S is the set of all cells of the given type, the partial duality relative to S is the total duality which swaps the two types of the remaining cells without changing the cells themselves and reverses the orientation of all cells in an oriented case.

For example, if hm is a graph cellularly embedded into a surface, then the total duality relative to the whole set of edges is the classical duality of graphs on surfaces which interchanges vertices and faces. Since the concept of hypermap is completely symmetrical, we can make the total duality relative to the set of vertices for example. Then, the edges and faces will be interchanged. The hypermap hm_1 from Fig. 7 has one vertex, one hyperedge, and three faces. Therefore, we have three total duals relative to the vertex, relative to the hyperedge, and relative to all three faces, which differ only by the colour (type) of the corresponding cells. In Fig. 9, the three duals are shown as cell decomposed spheres together with the corresponding embeddings of the hypergraphs; the hyperedges are embedded as one-dimensional stars centered at little squares.

The left picture represents $hm_1^{\{v\}}$ and has three hyperedges with a single half-edge each. The middle picture represents $hm_1^{\{e\}}$ with a single hyperedge of valency 3 adjacent to 3 distinct vertices and a single face. The right picture $hm_1^{\{f_1, f_2, f_3\}}$ is isomorphic to the original hypermap hm_1 .

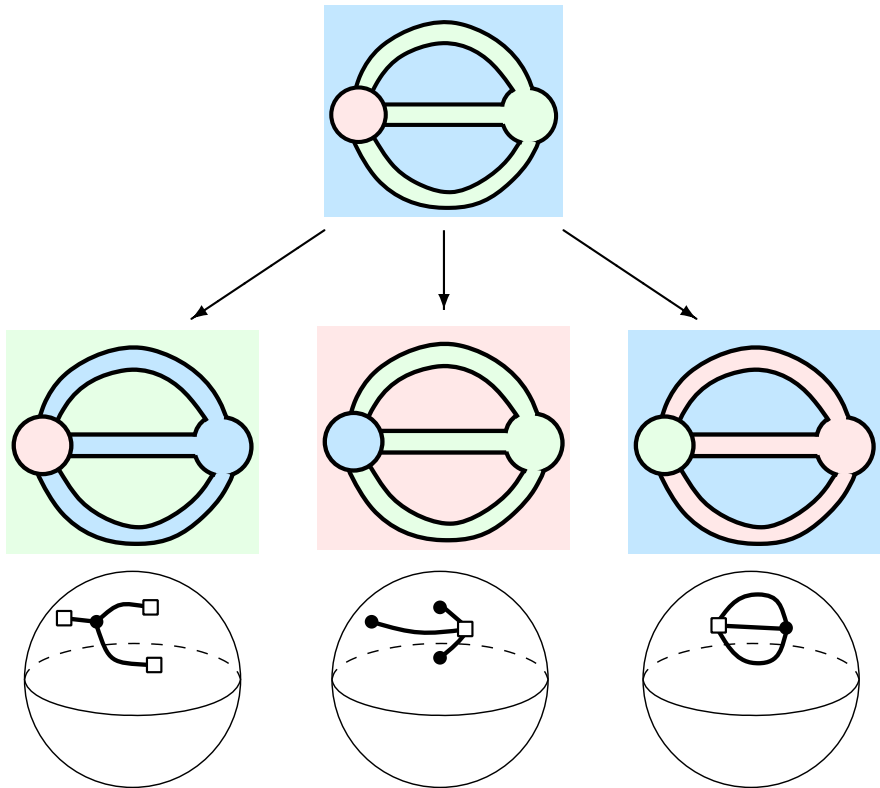


Fig. 9 Total duals of the hypermap $\mathfrak{h}m_1$ from Fig. 7

Definition 2.1 Without loss of generality, we may assume that S is a subset of the set of vertex-cells. Choose a different type of cells, say hyperedges. Later, in Lemma 2.2, we show that the resulting hypermap does not depend on this choice; we could choose faces instead of hyperedges if we want to.

Step 1. Consider the boundary ∂F of the surface F which is the union of the cells from S and all cells of the chosen type, hyperedges in our case.

Step 2. Glue a disk to each connected component of ∂F . These will be the *hyperedge-cells* for $\mathfrak{h}m^S$. Note that we do not include the interior of F into the hyperedges. Although if ∂F has only one component, gluing a disk to it results in the surface F itself, and then, we may consider F as the single hyperedge of $\mathfrak{h}m^S$. See Fig. 10.

Step 3. Take a copy of every vertex. These disks will be the *vertex-cells* for $\mathfrak{h}m^S$. Their attachment to the hyperedges is as follows. Every vertex-disk of the original hypermap $\mathfrak{h}m$ contributes one or several intervals to ∂F . Indeed, if a vertex belong to S , then it contributes to F itself and a part of its boundary contributes to ∂F . If a vertex is not in S , then it has some hyperedges attached to it, because $\mathfrak{h}m$ is assumed to be connected. Therefore, such a vertex-disk has a common boundary intervals with F and therefore contributes these intervals to ∂F . The new copies of the vertex-disks,

as vertices of $\mathfrak{h}\mathfrak{m}^S$, are attached to hyperedges exactly along the same intervals as the old ones. See Fig. 11.

Step 4. At the previous steps, we constructed the vertex and hyperedge-cells for the partial dual $\mathfrak{h}\mathfrak{m}^S$. Their union forms a surface with boundary. Glue a disk to each of its boundary components. These are going to be the *faces* of $\mathfrak{h}\mathfrak{m}^S$. See Fig. 12.

This finishes the construction of the partial dual hypermap $\mathfrak{h}\mathfrak{m}^S$.

Partial duality of hypermaps thus defined is a generalization of partial duality for maps [3]. Both indeed coincide on maps.

Example 3 We exemplify the construction of the partial dual $m_1^{\{v\}}$ for the map m_1 from fig. 7 relative to its left vertex v .

Similarly, one may find the partial dual $m_0^{\{v\}}$ for the non orientable map m_0 from Fig. 2. The resulting surface after step 3 will be similar to the one above, only one half-edge will be twisted. It still has one boundary component, and therefore a single face. Therefore, its Euler characteristic is still -2 ; only now the resulting hypermap will be non orientable. It represents a surface homeomorphic to a connected sum of 4 copies of the projective plane.

Lemma 2.2 *The resulting hypermap does not depend on the choice of type at the beginning of Definition 2.1.*

Proof Decompose the boundary circles of faces on a hypermap $\mathfrak{h}\mathfrak{m}$ into the union of three sets of arcs intersecting only at the end points of the arcs, $D_0(\mathfrak{h}\mathfrak{m}) \cup D_{1,S}(\mathfrak{h}\mathfrak{m}) \cup D_{1,\bar{S}}(\mathfrak{h}\mathfrak{m})$. The set $D_0(\mathfrak{h}\mathfrak{m})$ consists of arc of intersection of faces with hyperedges, $D_{1,S}(\mathfrak{h}\mathfrak{m})$ —of faces with vertices from the set S , and $D_{1,\bar{S}}(\mathfrak{h}\mathfrak{m})$ —of faces with vertices not from S . Analyzing the result of Step 3 of the construction, one can easily note that

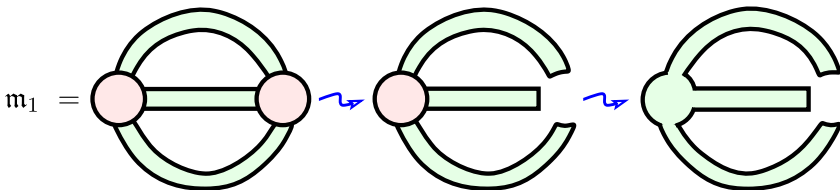


Fig. 10 Steps 1 & 2: forming hyperedges of $m_1^{\{v\}}$

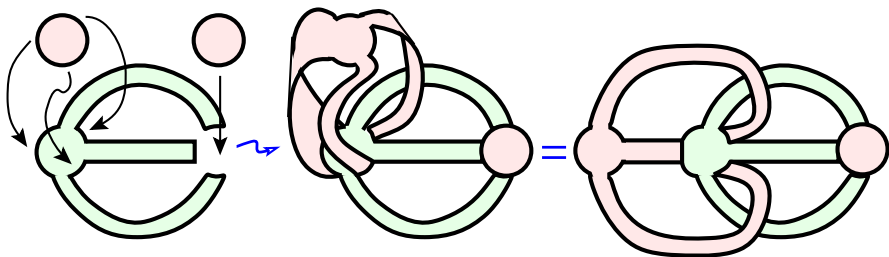


Fig. 11 Step 3: copying vertices and gluing them to hyperedges

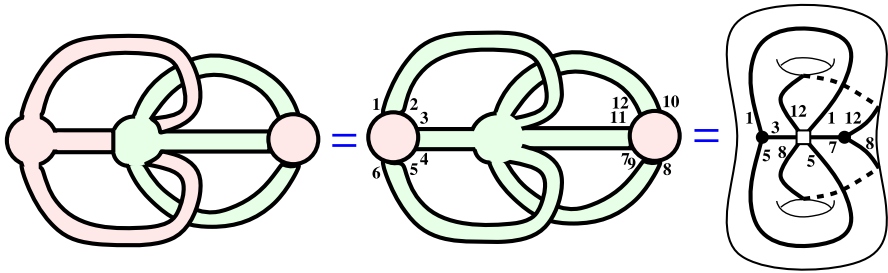


Fig. 12 Step 4: gluing faces and the resulting hypermap $m_1^{[v]}$

$D_0(\mathfrak{h}\mathfrak{m}) = D_0(\mathfrak{h}\mathfrak{m}^S)$ and $D_{1,S}(\mathfrak{h}\mathfrak{m}) = D_{1,S}(\mathfrak{h}\mathfrak{m}^S)$. Moreover, $D_{1,S}(\mathfrak{h}\mathfrak{m}^S)$ consists of the complementary arcs of the boundary circles of vertices from S to the arcs $D_{1,S}(\mathfrak{h}\mathfrak{m})$; formally, the complementary arcs on the second copies of the vertices of S . This means that the boundary circles of faces of $\mathfrak{h}\mathfrak{m}^S$ are exactly the boundary circles of the surface obtained by the union of vertices of S and all the faces. In other words on Step 1, we may take faces instead of hyperedges and we will get the same boundary circles as for $\mathfrak{h}\mathfrak{m}^S$. Then, by symmetry, the hyperedges will also be the same. \square

Analogously to [3, Sec.1.8], the following lemma describes simple properties of the partial duality for hypermaps. Its proof is obvious.

Lemma 2.3 (a) $(\mathfrak{h}\mathfrak{m}^S)^S = \mathfrak{h}\mathfrak{m}$.

(b) *There is a bijection between the cells of type S in $\mathfrak{h}\mathfrak{m}$ and the cells of the same type in $\mathfrak{h}\mathfrak{m}^S$. This bijection preserves the valency of cells. The number of cells of other types may change.*

(c) *If $s \notin S$, but has the same type as the cells of S , then $\mathfrak{h}\mathfrak{m}^{S \cup \{s\}} = (\mathfrak{h}\mathfrak{m}^S)^{\{s\}}$.*

(d) $(\mathfrak{h}\mathfrak{m}^{S'})^{S''} = \mathfrak{h}\mathfrak{m}^{\Delta(S', S'')}$, where $\Delta(S', S'') := (S' \cup S'') \setminus (S' \cap S'')$ is the symmetric difference of sets.

(e) *Partial duality preserves orientability of hypermaps.*

2.2 Partial Duality in σ -Model

For an oriented hypermap $\mathfrak{h}\mathfrak{m}$ represented in the σ -model of Sect. 1.3, we shall write

$$\mathfrak{h}\mathfrak{m} = (\sigma_V, \sigma_E, \sigma_F).$$

Theorem 2.4 *Let S be a subset $S := V'$ of vertices (resp. subset of hyperedges $S := E'$ and subset of faces $S := F'$) of a hypermap $\mathfrak{h}\mathfrak{m}$. Then, its partial dual is given by the permutations*

$$\mathfrak{h}\mathfrak{m}^{V'} = (\sigma_{\overline{V'}} \sigma_{V'}^{-1}, \sigma_E \sigma_{V'}, \sigma_{V'} \sigma_F)$$

$$\mathfrak{h}\mathfrak{m}^{E'} = (\sigma_{E'} \sigma_V, \sigma_{\overline{E'}} \sigma_{E'}^{-1}, \sigma_F \sigma_{E'})$$

$$\mathfrak{h}\mathfrak{m}^{F'} = (\sigma_V \sigma_{F'}, \sigma_{F'} \sigma_E, \sigma_{\overline{F'}} \sigma_{F'}^{-1}),$$

where $\sigma_{V'}$, $\sigma_{E'}$, $\sigma_{F'}$ denote the permutations consisting of the cycles corresponding to the elements of V' , E' , F' , respectively, and overline means the complementary set of cycles.

Similar formulas in the particular case of maps were announced in [14] (see also [13, Section 5.2]).

Proof Because of the symmetry, it is sufficient to prove the theorem in the case $S = V'$. From Definition 2.1, it follows that the number of half-edges is preserved by the partial duality. We need to make a bijection between half-edges of $\mathfrak{h}m$ and those of $\mathfrak{h}m^S$, such that the corresponding permutations are related as in the first equation of the theorem.

Half-edges are attached to vertices. If a vertex does not belong to S , then the attachment of half-edges to it does not change with partial duality (Step 2). Therefore, for those half-edges, the required bijection is the identity.

Half-edges attached to vertices of S change, so we need to indicate the bijection for them. Consider a vertex-disk from the set S of the original hypermap $\mathfrak{h}m$. It can be represented as a $2k$ -gon, because the arcs of its boundary circle intersecting with hyperedges and faces alternate. In $\mathfrak{h}m$, it has k half-edges attached along every other side. We call them *old half-edges*. These half-edges together with the vertex-disk form a piece of the surface F on Step 1 near the vertex. The orientation of F induces an orientation on its boundary ∂F . In the partial dual $\mathfrak{h}m^S$, the hyperedges, the *new hyperedges*, are attached to every connected component of ∂F (Step 2). The orientation of ∂F induces the orientation on new hyperedges. They are attached to a new vertex (Step 3) along the other sides of the $2k$ -gon, which form *new half-edges*. Set the label of a new half-edge to be the same as the label of the old one preceding the new half-edge in the direction of the orientation of the old vertex. This gives the bijection of half-edges around vertices of S . The orientation on the new vertex, as well as on the entire hypermap $\mathfrak{h}m^S$, is induced from the new hyperedges.

Figure 13 shows that the labels of the new half-edges appear around new vertices in the order opposite to the one around old ones. This means that the cycle in the permutation σ_V corresponding to a vertex in S of the initial hypermap $\mathfrak{h}m$ should be

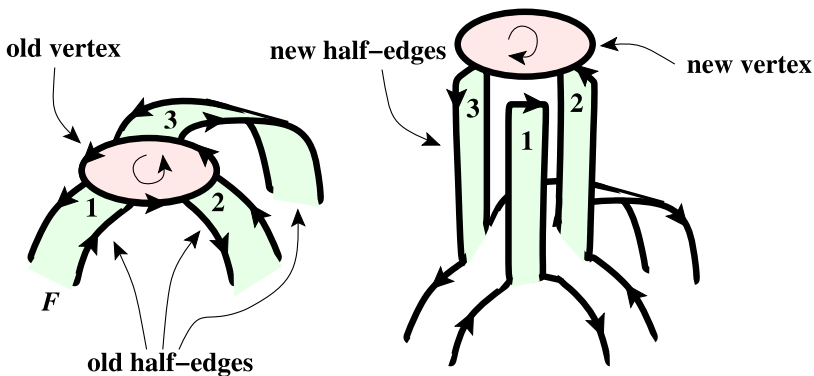


Fig. 13 Permutation $\sigma_V(\mathfrak{h}m^S)$

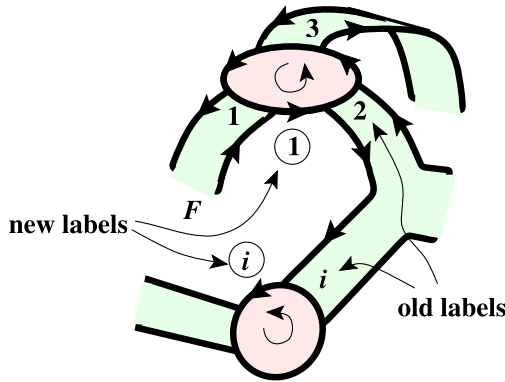


Fig. 14 Permutation $\sigma_E(\mathfrak{h}m^S)$

inverted to get the cycle for $\mathfrak{h}m^S$. This proves that the first term of the first formula of the theorem $\sigma_V(\mathfrak{h}m^S) = \sigma_{V'}^{-1}(\mathfrak{h}m)\sigma_{\overline{V'}}(\mathfrak{h}m)$.

For the second term, we need to analyze the cyclic order of new half-edges around new hyperedge according to its orientation. It may be read off from labels of the half-edges met when traveling along the boundary of the hyperedge in the direction of its orientation. Such a boundary for $\mathfrak{h}m^S$ is exactly a connected component of ∂F with the orientation induced from $\mathfrak{h}m$. The last is given precisely by the product of permutations $\sigma_E(\mathfrak{h}m)\sigma_{V'}(\mathfrak{h}m)$. Indeed, consider Fig. 14 and suppose that $\sigma_E(\mathfrak{h}m) : 2 \mapsto i$ for some i . Then, the new half-edge labels appear at ∂F in the order $\dots, 1, i, \dots$. So $\sigma_E(\mathfrak{h}m^S) : 1 \mapsto i$, which is equal to $\sigma_E(\mathfrak{h}m)\sigma_{V'}(\mathfrak{h}m)$

$$1 \xrightarrow{\sigma_{V'}(\mathfrak{h}m)} 2 \xrightarrow{\sigma_E(\mathfrak{h}m)} i .$$

This proves the second term.

The third term follows from the relation $\sigma_F\sigma_E\sigma_V = 1$. □

Example 4 This is a continuation of Example 1. We found that for the map m_1 in Fig. 7, the permutations σ 's act on the set of half-edges $H = \{1, 3, 5, 7, 8, 12\}$ as

$$\sigma_V = (1, 3, 5)(7, 8, 12), \quad \sigma_E = (1, 7)(3, 12)(5, 8), \quad \sigma_F = (1, 12)(3, 8)(5, 7).$$

The cycle $(1, 3, 5)$ of σ_V corresponds to the the left vertex v .

For the σ -model of the partial dual $m_1^{\{v\}}$, we set $V' = \{v\}$. Then, $\sigma_{V'} = (1, 3, 5)$ and $\sigma_{\overline{V'}} = (7, 8, 12)$. According to the theorem

$$\begin{aligned} \sigma_V(m_1^{\{v\}}) &= \sigma_{\overline{V'}}\sigma_{V'}^{-1} = (1, 5, 3)(7, 8, 12), \\ \sigma_E(m_1^{\{v\}}) &= \sigma_E\sigma_{V'} = (1, 7)(3, 12)(5, 8)(1, 3, 5) = (1, 12, 3, 8, 5, 7), \\ \sigma_F(m_1^{\{v\}}) &= \sigma_{V'}\sigma_F = (1, 3, 5)(1, 12)(3, 8)(5, 7) = (1, 12, 3, 8, 5, 7). \end{aligned}$$

One may check that these permutations agree with the last picture in Figs. 12 and 15.

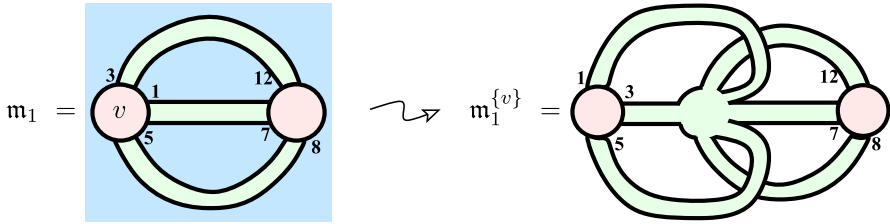


Fig. 15 Partial duality in σ -model

Corollary 2.5 *The total duality with respect to $S := V$ (resp. $S := E$ and $S := F$) is reduced to the classical Euler–Poincaré duality which swaps the names of two remaining types of cells and reverse the orientation.*

In σ -model, it is given by the formulae

$$\begin{aligned} \mathfrak{h}m^V &= (\sigma_V^{-1}, \sigma_E\sigma_V, \sigma_V\sigma_F) = (\sigma_V^{-1}, \sigma_F^{-1}, \sigma_E^{-1}) \\ \mathfrak{h}m^E &= (\sigma_E\sigma_V, \sigma_E^{-1}, \sigma_F\sigma_E) = (\sigma_F^{-1}, \sigma_E^{-1}, \sigma_V^{-1}) \\ \mathfrak{h}m^F &= (\sigma_V\sigma_F, \sigma_F\sigma_E, \sigma_F^{-1}) = (\sigma_E^{-1}, \sigma_V^{-1}, \sigma_F^{-1}). \end{aligned}$$

The inverse of these permutations is responsible for the change of orientation of the hypermap.

2.3 Partial Duality in τ -Model

Theorem 2.6 *Consider the τ -model of a hypermap $\mathfrak{h}m$ given by the permutations*

$$\begin{aligned} \tau_0(\mathfrak{h}m) &: (v, e, f) \mapsto (v', e, f), & \tau_1(\mathfrak{h}m) &: (v, e, f) \mapsto (v, e', f), \\ \tau_2(\mathfrak{h}m) &: (v, e, f) \mapsto (v, e, f') \end{aligned}$$

of its local flags. Let V' be a subset of its vertices, $\tau_1^{V'}$ be the product of all transpositions in τ_1 for $v \in V'$, and $\tau_2^{V'}$ be the product of all transpositions in τ_2 for $v \in V'$. Then, its partial dual $\mathfrak{h}m^{V'}$ is given by the permutations

$$\tau_0(\mathfrak{h}m^{V'}) = \tau_0, \quad \tau_1(\mathfrak{h}m^{V'}) = \tau_1\tau_1^{V'}\tau_2^{V'}, \quad \tau_2(\mathfrak{h}m^{V'}) = \tau_2\tau_1^{V'}\tau_2^{V'}.$$

In other words, the permutations τ_1 and τ_2 swap their transpositions of local flags around the vertices in V' . Similar statements hold for partial dualities relative to the subsets of hyperedges E' and of faces F' .

A particular case of these formulas for maps was rediscovered in [15, Equation 14] and announced in [14] (see also [13, Section 5.2]).

Proof From Definition 2.1, one may see that if a vertex does not participate in the partial duality, $v \notin V'$, then nothing changes with local flags around it. However, if

$v \in V'$, then the roles of edges and faces in its local flags are interchanged. This may be seen on Step 3 and also in Figs. 13, and 14 when the second copy of the vertex is attached to the new hyperedges. Therefore, if two such local flags were transposed by τ_1 of the original hypermap, then they will be transposed by τ_2 of the partial dual and vice versa. □

Example 5 In Example 1, we found the τ -model for the map m_1 of Fig. 7

$$\begin{aligned} \tau_0 &= (1, 11)(2, 12)(3, 10)(4, 8)(5, 9)(6, 7), & \tau_1 &= (1, 2)(3, 4)(5, 6)(7, 9)(8, 10)(11, 12), \\ \tau_2 &= (1, 6)(2, 3)(4, 5)(7, 11)(8, 9)(10, 12). \end{aligned}$$

There are six flags around the left vertex v labeled by $1, 2, \dots, 6$. The corresponding transpositions around this vertex are

$$\tau_1^{\{v\}} = (1, 2)(3, 4)(5, 6), \quad \tau_2^{\{v\}} = (1, 6)(2, 3)(4, 5).$$

Swapping them between τ_1 and τ_2 , we get the τ -model of the partial dual

$$\begin{aligned} \tau_0(\mathfrak{h}m^{\{v\}}) &= (1, 11)(2, 12)(3, 10)(4, 8)(5, 9)(6, 7), \\ \tau_1(\mathfrak{h}m^{\{v\}}) &= (1, 6)(2, 3)(4, 5)(7, 9)(8, 10)(11, 12), \\ \tau_2(\mathfrak{h}m^{\{v\}}) &= (1, 2)(3, 4)(5, 6)(7, 11)(8, 9)(10, 12). \end{aligned}$$

This agrees with the labeling of flags on Figs. 12 and 16.

Corollary 2.7 *The τ -model of the total dual $\mathfrak{h}m^V$ of a hypermap $\mathfrak{h}m$ is given by the involutions*

$$\tau_0(\mathfrak{h}m^V) = \tau_0(\mathfrak{h}m), \quad \tau_1(\mathfrak{h}m^V) = \tau_2(\mathfrak{h}m), \quad \tau_2(\mathfrak{h}m^V) = \tau_1(\mathfrak{h}m).$$

One may check that this agrees with Corollary 2.5 in the case of oriented hypermaps.

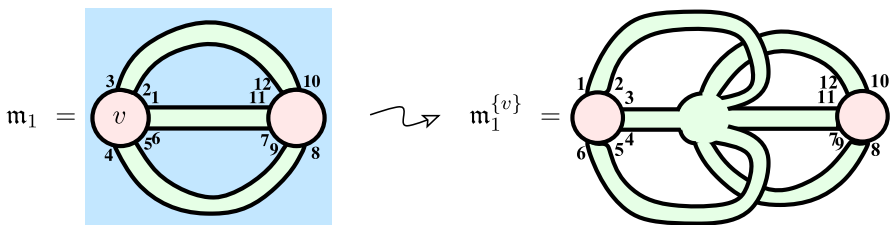


Fig. 16 Partial duality in τ -model

2.4 Partial Duality for Coloured Graphs

Let $\Gamma_{\mathfrak{h}_m}$ be the [2]-coloured graph corresponding to a hypermap \mathfrak{h}_m . Let I be a subset of two out of three colours, for example $I = \{1, 2\}$, and let S be a subset of 2-bubbles in \mathcal{B}^I which corresponds to a subset of vertices of \mathfrak{h}_m .

Theorem 2.8 *The [2]-coloured graph $\Gamma_{\mathfrak{h}_m^S}$ of the partial dual hypermap \mathfrak{h}_m^S is obtained from $\Gamma_{\mathfrak{h}_m}$ by swapping the colours 1 and 2 for all edges in the 2-bubbles of S . In particular, the underlying graphs of $\Gamma_{\mathfrak{h}_m^S}$ and $\Gamma_{\mathfrak{h}_m}$ are the same.*

Ellingham and Zha [11] obtained a similar result in the case of maps.

Proof The edges of $\Gamma_{\mathfrak{h}_m}$ of colour 1 (resp. 2) correspond to 2-element orbits of τ_1 (resp. τ_2). According to Theorem 2.6, the partial dual hypermap is obtained by swapping the corresponding transpositions of τ_1 and τ_2 . This corresponds to swapping the colours 1 and 2 in the bubbles of S . □

Example 6 Here are the [2]-coloured graphs $\Gamma_{\mathfrak{h}_m^V}$, $\Gamma_{\mathfrak{h}_m^E}$ and $\Gamma_{\mathfrak{h}_m^F}$ for the total duals of the hypermap \mathfrak{h}_m from Fig. 7 relative to the set of all vertices V , all edges E , and all faces F . These dual hypermaps are shown in Fig. 9.

Remark (Higher dimensional partial duality) Such an easy interpretation of partial duality for [2]-coloured graphs easily allows to make a higher dimensional generalization to $[D]$ -coloured graphs Γ . Namely, fix a set I of D colours out of the total number of $D + 1$ colours, and let S be a subset of D -bubbles in \mathcal{B}^I . The *partial dual* Γ^S relative to S is a $[D]$ -coloured graph obtained from Γ by a permutation of the colours of the edges in S .

In this case, the word “duality” is inappropriate. It is rather an action of a symmetric group S_D on colours of edges of bubbles of S . In the hypermap case, $D = 2$. This group is isomorphic to \mathbb{Z}_2 , so the partial duality corresponds to the only nontrivial element of order 2. However, for higher D , the group S_D contains higher order elements, so they will not be “dualities” anymore (Fig. 17).

This concept of higher dimensional partial duality is completely unexplored up to now. It would be very interesting to study it. In particular, is it true that if the realization $|\Gamma|$ of Γ through its direct complex $\Delta(\Gamma)$ is a manifold, then the realization of its partial dual $|\Gamma^S|$ is also a manifold? How partial duality affects the (co)homology groups $H_*(\Delta(\Gamma))$?

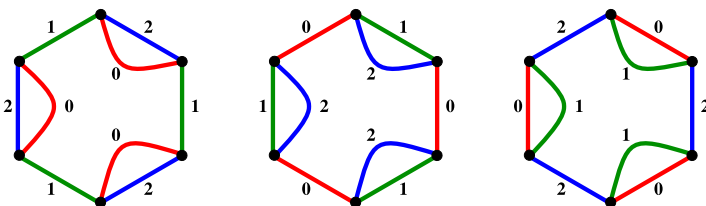


Fig. 17 [2]-Coloured graphs of total duals $\Gamma_{\mathfrak{h}_m^V}$, $\Gamma_{\mathfrak{h}_m^E}$, $\Gamma_{\mathfrak{h}_m^F}$

3 Genus Change

The *Euler genus* γ is equal to twice the genus for orientable hypermaps and to the number of Möbius bands μ in presentations of the surfaces of hypermaps as spheres with μ bands in them in the unorientable case. The bijection between hypermaps and [2]-coloured graphs, see Sect. 1.4.2, allows us to derive a simple formula for the Euler genus change under partial duality, in terms of change of the numbers of bicoloured cycles (or 2-bubbles). In the case of maps, it expresses the genus change in terms of certain induced subgraphs of the map and of its total dual.

Definition 3.1 (Special subgraphs) Let Γ be a [2]-coloured graph and C be a subset of $\mathcal{B}^{(i,j)}(\Gamma)$, $i, j \in [2]$ relative to which we are going to do the partial duality. Let k denote the unique element of $[2] \setminus \{i, j\}$. For all $t \in [2]$, we define

- $\bar{\Gamma}[C; tk]$ as the (possibly disconnected) edge-coloured subgraph of Γ made of the cycles in C and all the tk -cycles incident with C ,
- $\Gamma_s[C; tk]$ as the (possibly disconnected) edge-coloured graph obtained from $\bar{\Gamma}[C; tk]$ by contracting (in the sense of coloured graphs) all the t -edges not in C . Therefore, every tk -path outside C will be replaced by a single edge of colour k .

An example is given in Fig. 18.

Recall the definition of I -bubbles in Definition 1.4.

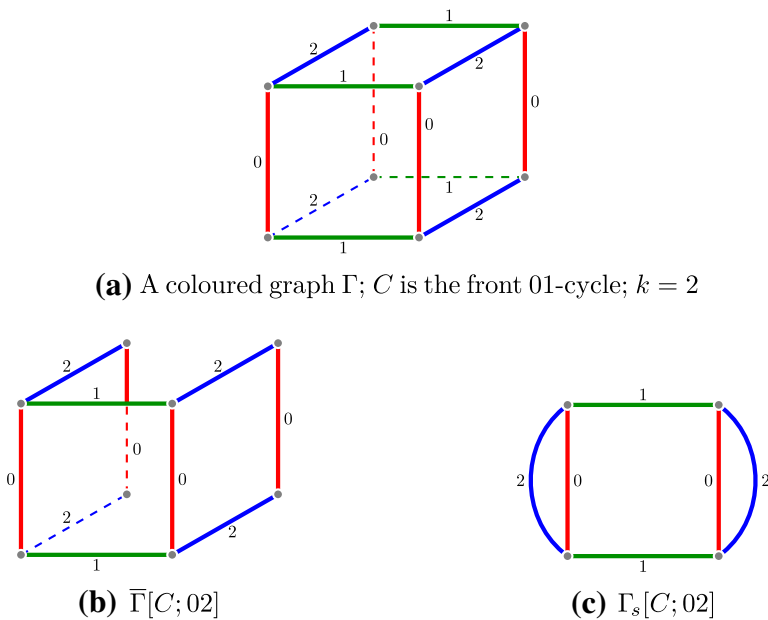


Fig. 18 Special subgraphs of coloured graphs

Lemma 3.2 *Let Γ, C, k and t be as in Sect. 3.1. Then*

$$\begin{aligned} \Delta_{tk}^C &:= B^{tk}(\Gamma^C) - B^{tk}(\Gamma) = B^{\{tk\}}(\Gamma_s[C; tk]) - B^{tk}(\Gamma_s[C; tk]) \\ &= -2B^{tk}(\Gamma_s[C; tk]) - \#C + n(\Gamma_s[C; tk]) - \gamma(\Gamma_s[C; tk]) + 2k(\Gamma_s[C; tk]), \end{aligned}$$

where $n(\Gamma_s[C; tk])$ is half of the number of vertices of $\Gamma_s[C; tk]$ and k denotes the number of connected components.

Proof Let \bar{t} be the unique element of $\{i, j\} \setminus \{t\}$. By definition

$$\begin{aligned} B^{tk}(\Gamma^C) - B^{tk}(\Gamma) &= B^{tk}(\Gamma_s^C[C; tk]) - B^{tk}(\Gamma_s[C; tk]) \\ &= B^{\{\bar{t}k\}}(\Gamma_s[C; tk]) - B^{tk}(\Gamma_s[C; tk]). \end{aligned} \tag{3.1}$$

The surface corresponding to a [2]-coloured graph Γ has Euler characteristic

$$\chi(\Gamma) = 2k(\Gamma) - \gamma(\Gamma) = B^{ij}(\Gamma) + B^{ik}(\Gamma) + B^{jk}(\Gamma) - n(\Gamma). \tag{3.2}$$

For $\Gamma = \Gamma_s[C; tk]$, we have $B^{ij}(\Gamma_s[C; tk]) = \#C$ and Eq. (3.2) gives

$$\begin{aligned} B^{\{\bar{t}k\}}(\Gamma_s[C; tk]) \\ = -B^{tk}(\Gamma_s[C; tk]) - \#C + n(\Gamma_s[C; tk]) - \gamma(\Gamma_s[C; tk]) + 2k(\Gamma_s[C; tk]). \end{aligned}$$

Substituting it into Eq. (3.1), one gets the desired result. □

Theorem 3.3 *Let Γ be a [2]-coloured graph and C be a subset of $\mathcal{B}^{i,j}(\Gamma)$. Let k be the unique element of $[2] \setminus \{i, j\}$. Then*

$$\gamma(\Gamma^C) - \gamma(\Gamma) = -\Delta_{ik}^C(\Gamma) - \Delta_{jk}^C(\Gamma),$$

where Δ_{ik}^C is given by Lemma 3.2.

Proof One simply uses Eq. (3.2) and remarks that $k(\Gamma^C) = k(\Gamma)$, $n(\Gamma^C) = n(\Gamma)$, and $B^{ij}(\Gamma^C) = B^{ij}(\Gamma)$. □

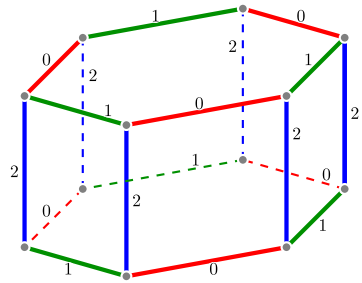
Remark Theorem 3.3 allows to derive bounds on $\gamma(\Gamma^C) - \gamma(\Gamma)$. For any $t \in \{i, j\}$ and any coloured graph Γ , the number of tk -cycles in $\Gamma_s[C; tk]$, $B^{tk}(\Gamma_s[C; tk])$ lies between 1 and $n(\Gamma_s[C; tk]) = \frac{1}{2} \sum_{c \in C} \text{length}(c)$. This gives

$$|\gamma(\Gamma^C) - \gamma(\Gamma)| \leq \sum_{c \in C} (\text{length}(c) - 2).$$

This bound is optimal and Fig. 19 shows an example where it is reached.

Given the bijection between hypermaps and [2]-coloured graphs, ribbon graphs are [2]-coloured graphs, the 02-cycles of which all have length four. Theorem 3.3 then applies and allows to quantify the change of topology of ribbon graphs under partial duality.

Fig. 19 A coloured graph Γ , such that $g(\Gamma^C) - g(\Gamma) = 2$, C is any of its 01-cycles



Corollary 3.4 *Let G be a ribbon graph and E' be a subset of its edges. Let $G[E']$ be the subribbon graph of G induced by E' and $G^*[E']$ be the subribbon graph of its Euler–Poincaré dual G^* induced by E' . Then*

$$\frac{1}{2}(\gamma(G^{E'}) - \gamma(G)) = v(G[E']) + v(G^*[E']) - \#E' - \frac{1}{2}\chi(G[E']) - \frac{1}{2}\chi(G^*[E']).$$

Proof With our conventions, $C = E'$ is a subset of 02-cycles, vertices are 12-cycles, and faces are 01-cycles. Thus, $\Gamma_s[E'; 12] = G[E']$, $\Gamma_s[E'; 01] = (G^*[E'])^*$, $n(\Gamma_s[E'; 1t]) = 2\#E'$, and the Corollary follows. \square

In particular, for partial duality of ribbon graphs relative to a single edge, $\#E' = 1$, Corollary 3.4 immediately gives the results of [13, Table 1.1] which were recently used in to prove one of the conjectures from [13].

4 Directions of Future Research

- The paper [13] contains several interesting conjectures about partial dual genus distribution polynomial for ribbon graphs. One of them was recently proved in [7]. The definition of this polynomial works for hypermaps, as well. It would be interesting to formulate and prove analogs for hypermaps.
- Maps (ribbon graphs) provide a special class of Δ -matroids (Lagrangian matroids) [4]. Are there any matroid type structure underlying the concept of hypermaps? Can the general Coxeter matroids be obtained from hypermaps?
- It would be interesting to study higher dimensional partial “duality” concept as outlined in Sect. 2.4. In particular, is it true that a partial “dual” to a $[D]$ -coloured graph corresponding to a manifold is also a manifold?

Acknowledgements We are grateful to Iain Moffatt and Neal Stoltzfus for fruitful discussions on our preliminary results during the Summer 2014 Programm “Combinatorics, geometry, and physics” in Vienna, and the Erwin Schrödinger International Institute for Mathematical Physics (ESI) and the University of Vienna for hospitality during the program. We also thank the anonymous referees for their constructive comments which helped clarify our exposition. S. Ch. thanks the Max-Plank-Institut für Mathematik in Bonn and the Université Lyon 1 for excellent working conditions and warm hospitality during the visits in 2014 and 2016. F. V.-T. is partially supported by the grant ANR JCJC CombPhysMat2Tens.

References

1. Bradford, R., Butler, C., Chmutov, S.: Arrow ribbon graphs. *J. Knot Theory Ramif.* **21**(13), 1240002 (2012). <https://doi.org/10.1142/S0218216512400020>. arXiv:1107.3237 [math.CO]
2. Cavicchioli, A., Grasselli, L., Pezzana, M.: Su di una decomposizione normale per le n -varietà chiuse. *Boll. Un. Mat. Ital.* **17B**, 1146–1165 (1980)
3. Chmutov, S.: Generalized duality for graphs on surfaces and the signed Bollobás–Riordan polynomial. *J. Comb. Theory Ser. B* **99**(3), 617–638 (2008). arXiv:0711.3490 [math.CO]
4. Chun, C., et al.: Matroids, delta-matroids and embedded graphs. *J. Comb. Theory Ser. A* **167**, 7–59 (2019). arXiv:1403.0920 [math.CO]
5. Coxeter, H.S.M., Moser, W.O.J.: *Generators and Relations for Discrete Groups*, 4th edn. Springer, Berlin (1980)
6. Cori, Robert. Un code pour les graphes planaires et ses applications. *Astérisque*, **27**, 178 (1975). http://numdam.org/item/AST_1975__27__1_0/
7. Chmutov, S., Vignes-Tourneret, F.: On a conjecture of gross, mansour and tucker. *Eur. J. Comb.* (2021). <https://doi.org/10.1016/j.ejc.2021.103368>. arXiv:2101.09319 [math.CO]
8. Edmonds, J.K.: A combinatorial representation for polyhedral surfaces. *Not. Am. Math. Soc.*, **7**, 646 (1960)
9. Ellis-Monaghan, J.A., Moffatt, I.: Twisted duality for embedded graphs. *Trans. Am. Math. Soc.* **364**(3), 1529–1569 (2010). <https://doi.org/10.1090/S0002-9947-2011-05529-7>. arXiv:0906.5557 [math.CO]
10. Ellis-Monaghan, J.A., Moffatt, I.: *Graphs on Surfaces. Dualities, Polynomials, and Knots*. Springer-Briefs in Mathematics, p. XI+139. Springer, Berlin (2013)
11. Ellingham, M.N., Zha, X.: Partial duality and closed 2-cell embeddings. *J. Comb.* **8**(2), 227–254 (2017). arXiv:1501.06043 [math.CO]
12. Ferri, M., Gagliardi, C., Grasselli, L.: A graph-theoretical representation of PL-manifolds: a survey on crystallizations. *Aequ. Math.* **31**, 121–141 (1986)
13. Gross, J.L., Mansour, T., Tucker, T.W.: Partial duality for ribbon graphs, I: distributions. *Eur. J. Comb.* **86**, 103084 (2020). <https://doi.org/10.1016/j.ejc.2020.103084>
14. Gross, J.L., Mansour, T., Tucker, T.W.: Partial duality for ribbon graphs, II: partial-twuality polynomials and monodromy computations. *Eur. J. Comb.* (2021). <https://doi.org/10.1016/j.ejc.2021.103329>
15. Gross, J.L., Tucker, T.W.: Enumerating graph embeddings and partial-duals by Genus and Euler Genus. *Enumer. Combin. Appl.* **1**(1) (2020)
16. Gurau, R.: Colored group field theory. *Commun. Math. Phys.* **304**, 69–93 (2010). <https://doi.org/10.1007/s00220-011-1226-9>. arXiv:0907.2582 [hep-th]
17. Gurau, R.: Lost in translation: topological singularities in group field theory. *Class. Quantum Gravity* (2010). <https://doi.org/10.1088/0264-9381/27/23/235023>. arXiv:1006.0714 [hep-th]
18. Heffter, L.: Über das Problem der Nachbargebiete. *Math. Ann.* **38**, 477–508 (1891)
19. Huggett, S., Moffatt, I.: Bipartite partial duals and circuits in medial graphs. *Combinatorica* **33**, 231–252 (2013). <https://doi.org/10.1007/s00493-013-2850-0>. arXiv:1106.4189 [math.CO]
20. James, L.D.: Operations on hypermaps, and outer automorphisms. *Eur. J. Comb.* **9**(6), 551–560 (1988)
21. Jones, G.A., Pinto, D.: Hypermap operations of finite order. *Discrete Math.* **310**(12), 1820–1827 (2009). arXiv:0911.2644
22. Jones, G.A., Thornton, J.S.: Operations on maps, and outer automorphisms. *J. Comb. Theory Ser. B* **35**(2), 93–103 (1983)
23. Klein, F.: *Lectures on the Icosahedron and the Solution of Equations of the Fifth Degree*. Translation of Vorlesungen über das Ikosaeder und die Auflösung der Gleichungen vom fünften Grade (1884). Dover Publications, New York (1956)
24. Kozlov, D.: *Combinatorial Algebraic Topology. Algorithms and Computation in Mathematics*, vol. 21. Springer, Berlin (2008)
25. Lins, S.: Graph-encoded maps. *J. Comb. Theory Ser. B* **32**(2), 171–182 (1982). [https://doi.org/10.1016/0095-8956\(82\)90033-8](https://doi.org/10.1016/0095-8956(82)90033-8)
26. Lins, S., Mandel, A.: Graph-encoded 3-manifolds. *Discrete Math.* **57**, 261–284 (1985)
27. Lando, S.K., Zvonkin, A.K.: *Graphs on Surfaces and Their Applications*. In: Gamkrelidze, R., Vassiliev, V. (eds.) *Encyclopaedia of Mathematical Sciences*, vol. 141. Springer, Berlin (2004)
28. Moffatt, I.: Partial duality and Bollobás and Riordan’s Ribbon graph polynomial. *Discrete Math.* **310**, 174–183 (2008). arXiv:0809.3014

29. Moffatt, I.: A characterization of partially dual graphs. *J. Graph Theory* **67**(3), 198–217 (2010). [arXiv:0901.1868](#)
30. Moffatt, I.: Separability and the genus of a partial dual. *Eur. J. Comb.* **34**(2), 355–378 (2012). [arXiv:1108.3526](#) [math.CO]
31. Pezzana, M.: Sulla struttura topologica delle varietà compatte. *Atti Sem. Mat. Fis. Univ. Modena* **23**, 269–277 (1974)
32. Pezzana, M.: Diagrammi di Heegaard e triangolazione contratta. *Boll. Un. Mat. Ital.* **12**(4), 98–105 (1975)
33. Smith, B.: Matroids, Eulerian Graphs and Topological Analogues of the Tutte Polynomial. Ph.D. thesis. Royal Holloway, University of London (2018)
34. Tutte, W.T.: Graph Theory. In: Rota, G.C. (ed.) *Encyclopedia of Mathematics and its Applications*, vol. 21. Addison-Wesley Publishing Company, Boston (1984)
35. Vince, A.: Combinatorial maps. *J. Comb. Theory Ser. B* **34**(1), 1–21 (1983)
36. Vince, A.: Map duality and generalizations. *Ars Comb.* **39**, 211–229 (1995)
37. Vignes-Tourneret, F.: The multivariate signed Bollobás–Riordan polynomial. *Discrete Math.* **309**, 5968–5981 (2009). <https://doi.org/10.1016/j.disc.2009.04.026>. [arXiv:0811.1584](#) [math.CO]
38. Walsh, T.R.S.: Hypermaps versus bipartite maps. *J. Comb. Theory Ser. B* **18**, 155–163 (1975)
39. Wilson, S.E.: Operators over regular maps. *Pac. J. Math.* **81**(2), 559–568 (1978)

Publisher's Note Springer Nature remains neutral with regard to jurisdictional claims in published maps and institutional affiliations.